

Microstructure and Wear Resistance of Laser Cladded Ni-based Coatings with Nanometer La_2O_3 Addition

Zhao Ning^{1,2}, Tao Li^{1,2}, Guo Hui^{1,2}, Zhang Mengqi^{1,2}

¹ Northwestern Polytechnical University, Xi'an 710072, China; ² Shaanxi Engineering Laboratory for Transmissions and Controls, Xi'an 710072, China

Abstract: Ni-based coatings with nano-sized feedstock rare earth element (RE, La_2O_3) addition were produced by laser cladding. Bed of high energy ball milling mixed Ni60A and La_2O_3 powders were pre-placed onto the substrate 30CrMnSiNi2A before laser cladding. Results show that La segregates in inter dendrite and thus secondary dendrites growth and ripening are limited. The microstructure is refined. Top surface of the cladded coatings displays better refined microstructure which is caused by high La concentration, and this phenomenon is verified in EPMA results. The cracks and pores cannot be found in cladded coatings in which microstructure refinement and purifying effect caused by RE is clearly reflected in SEM microstructure, hardness and especially the wear resistance test results. The COF (coefficient of friction) of the coatings is apparently lower than that of substrate steel; the wear volume loss rate and the microhardness of coatings are less than 1/10 and about 4 times higher than that of substrate metal, respectively. This research forms the basement of metal surface anti-wear layer on the work surface of high speed heavy duty gear set in helicopter transform system.

Key words: Ni-based alloy coating; La_2O_3 ; laser clad; microstructure refinement; abrasive wear

Ni-based self-fluxing alloys are extensively used to produce abrasive resistance coatings^[1-14]. Nickel based alloy coatings combine excellent properties such as good corrosion resistance and low wear loss rate, and hard particles usually added in Ni-based alloy coatings are lanthanum oxide^[7,8], samarium oxide^[9], cerium oxide^[10,11], yttrium oxide^[12-15], $\text{WC}^{[1,4-6,8]}$ and $\text{TiC}^{[12]}$. RE added in Ni-based alloys is aimed at solid solution strengthening, microstructure refinement and structural purifying as well as corrosion resistance^[7-11]. The mechanical properties such as coating hardness, wear, corrosion resistance and toughness of laser coatings can be improved by RE addition^[7-15]. Song et al^[16] found that the Ce-doped sample showed grain boundary segregation in heat-affected zones (HAZ) and made finer microstructure than the Ce-undoped sample. Serres et al^[17] discovered that in situ laser remelting can produce dense coatings which have high fracture toughness, mean contact pressure and Young's modulus.

The La_2O_3 and CeO_2 addition in laser cladded NiCrBSi coatings has been reported^[7,18]. Yet to the best of the authors' knowledge literature did not reveal any research about laser cladded Ni based coatings added with nanometer La_2O_3 on ultra-high strength steel.

In view of the above an attempt in the present study has been made to systematically analyze laser cladded Ni- La_2O_3 coatings. Particularly, the role of lanthanum oxide on microstructure dendrite refinement and wear behaviors of Ni-based alloy coatings were investigated. This study lays foundation for surface reinforcement of high speed heavy load gear set.

1 Experiment

Super high strength steel 30CrMnSiNi2A (11 mm×161.2 mm×49.8 mm) was used as substrate and the chemical composition of substrate steel and commercially available

Received date: August 24, 2016

Foundation item: National Natural Science Foundation of China (51075328, 51675424); the Fundamental Research Funds for the Central Universities (3102015BJ (II) MYZ28)

Corresponding author: Tao Li, Candidate for Ph. D., School of Mechatronics, Northwestern Polytechnical University, Xi'an 710072, P. R. China, E-mail: taoli0401@163.com

Copyright © 2017, Northwest Institute for Nonferrous Metal Research. Published by Elsevier BV. All rights reserved.

Ni60A powder is listed in Table 1. Ni60 powder was modified with 1.2 wt% La₂O₃. The purity and average particle size of La₂O₃ used in this study are 99.7% and 4 nm. The powder mixture of Ni60 and nano-La₂O₃ was clad by CO₂ laser (CP4000, Convergent) with shielding gas nitrogen. Laser process parameters are listed in Table 2.

The as-clad specimen were cut, ground and mechanical polished on struers tegrapol-25 (Struers, Denmark) before the microstructure characterization by field emission scanning electron microscope (FSEM, Quanta 600FEG, FEI) and their phases constitution identification by X-ray diffraction (XRD, DX-2700) with Cu K α as a radiation, $\lambda=0.154\ 056\ \text{nm}$, step of 0.02° ; the scanning $2\theta=20^\circ\sim 100^\circ$. The elements content quantification was conducted by electron probe micro-analyzer (EPMA-1720). Reciprocating dry sliding wear test was performed on wear instrument (UMT, Cetr). Optical 3D worn surface metrology was conducted on 3D profilometer (Uscan Custom, Nanofocus) to figure out abrasive wear volume loss rate of Ni-La₂O₃ coatings, un-coated substrate metal 30CrMnSi Ni2A and their counterpart GCr15 balls.

2 Results

2.1 Microstructure of the as-received coating

Fig.1 shows the SEM micrograph of coatings cross section. It is clear that the microstructure of the clad coatings is uniform and compact dendrite grains and eutectics without any macro cracks or pores. The coating surface is neat and flat. The main grain morphology in the top area is dendrite of about $1\ \mu\text{m}$ in size as shown in Fig.2. Along the depth, the grain morphology gradually increases from coating surface to middle. It is found that in the middle region, the average diameter of γ -(Ni, Fe) solid-solution is about $3\ \mu\text{m}$, larger than $1\ \mu\text{m}$ for dendrites diameter in top region. The formation of fine dendrites by rare earth (RE) element in Ni-based alloy is thought to be a beneficial mechanism^[14,15]. La segregates in interdendrite. Therefore, the γ -(Ni, Fe) solid-solution and eutectic growth are limited.

EPMA line scanning analysis of La interdendrite distribution is shown in Fig.3. It is clear that La mainly exists in γ -(Ni, Fe) interdendrite. Thus the constraint of secondary dendrite ripening and coarsening is caused by La.

Table 1 Chemical composition of the substrate and Ni alloy powders (wt%)

Element	30CrMnSiNi2A	Ni60A
Ni	1.40~1.80	Bal.
Fe	Bal.	≤ 6.0
C	0.27~0.34	0.8
Si	1.20	4.0
Mn	1.00~1.30	-
S	≤ 0.02	-
P	≤ 0.02	-
Cr	0.90~1.20	17.0
B	-	3.5

Table 2 Parameters for laser cladding

Process parameters	Operation range
Laser type	CO ₂
Laser power/kW	1.5~2
Laser beam diameter/mm	~ 2
Melt pool diameter/mm	~ 3
Traverse speed/mm s ⁻¹	8
Overlap rate/%	25

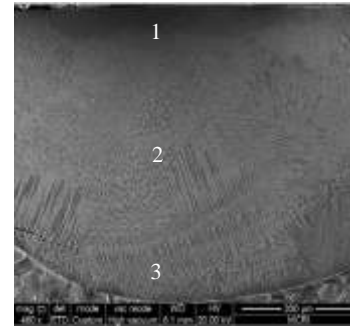


Fig.1 SEM image of coating surface cross section

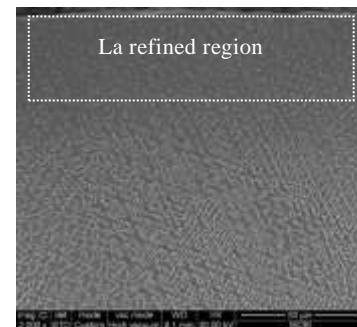


Fig.2 Top surface zone of La reduced dendrite size

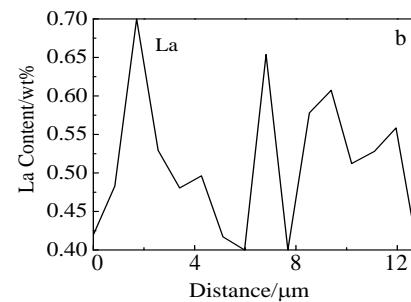
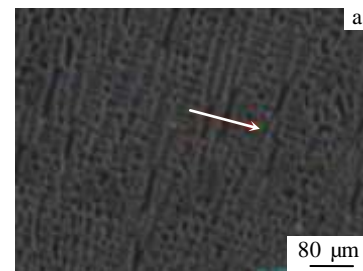


Fig.3 EPMA line scanning analysis of location map (a) and La content (b)

A high magnification graph of phase identification of coating cross section labeled 1~3 are shown in Fig.4. Based on the EDS and XRD result of Table 3 and Fig.5, addition to the primary phases γ -(Ni, Fe), the white angular carbide particle blocks labeled 1, 2 indicate the degenerate carbide M_7C_3 , which is mainly Cr_7C_3 , and the gray typical laminar eutectic area labeled 3 is $(\gamma$ -(Ni, Fe)+ $M_{23}C_6$) eutectic. The majority of M in $M_{23}C_6$ is Cr.

Observation on phases was conducted by XRD. According to Fig.5, the coating mainly consists of Ni and Fe solid solution, Cr_7C_3 , $Cr_{23}C_6$ and Cr_2Ni_3 . The carbides are helpful in hardness improvement of Ni-based alloy coatings.

2.2 Wear resistance

It is clear in Fig.6 that the hardness of both coating and HAZ are obviously higher than that of the substrate. The average microhardness of coatings and HAZ are 3~4 times greater than that of the substrate. Effect of grain boundary strengthening and solid-solution strengthening in Ni-alloy can be brought by proper rare earth element addition^[14]. La segregates to solid/liquid interface during solidification to inhibit the crystal growth and promote dendrite refinement. Rare earth element in Ni, Fe-based alloy melt pool react easily with sulfur and the sulfide is floatable and prone to float to the top surface of composite coatings. Hence the

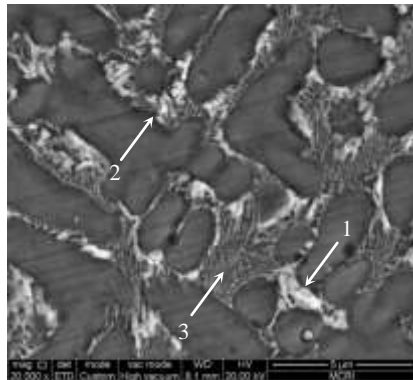


Fig.4 SEM image of coating top surface high magnification phase indication

Table 3 EDS quantification analysis of locations labeled 1-3 in Fig.4 (at%)

Element	Label 1	Label 2	Label 3
B	24.50	22.64	19.19
C	38.07	37.80	31.81
O	3.92	6.22	5.01
Si	3.59	4.30	4.81
Cr	4.24	4.07	5.33
Fe	19.58	19.61	25.88
Ni	5.54	4.93	7.27
La	0.55	0.44	0.60

content of sulfur remained in melt is decreased, which in turn increases the materials strength of coating alloy^[15].

The coefficient of friction (COF) curves of coating specimens and substrate metal without laser clad coatings in Fig.7 show that the COF of Ni60A-La₂O₃ coatings is lower and the average value is about 0.56 under dry sliding condition.

Fig.8 shows the result of wear volume loss measurement of un-coated substrate and as-clad coating specimens and their wear counterparts GCr15 ball. The wear volume loss rate value of Ni60A-La coatings and substrate metal

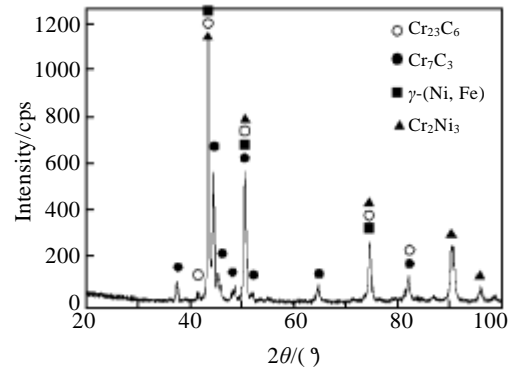


Fig.5 XRD pattern of the top surface of the composite coating

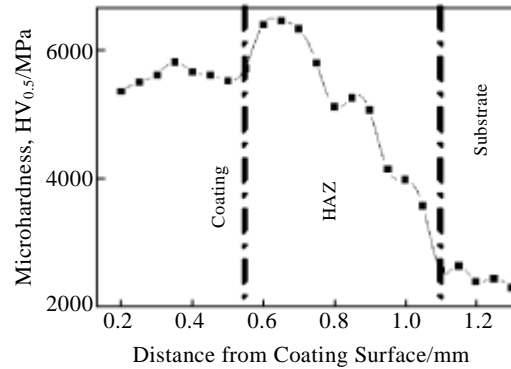


Fig.6 Microhardness of single track zone

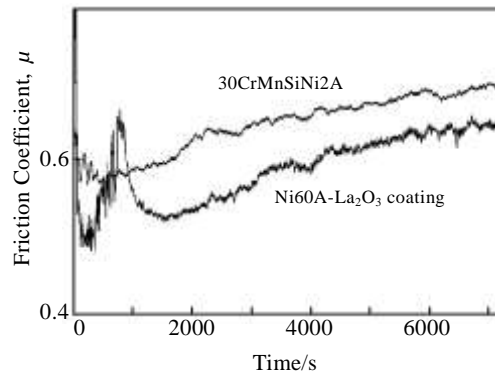


Fig.7 Friction coefficient of substrate and coating specimens

are 1 and 13.5, and the values of their GCr15 balls are almost identical, 44.8 and 44, respectively.

In Fig.9, laser reheating reforms a smaller austenite grain size HAZ beneath the coating/substrate interface, refining HAZ grain size and increasing the hardness. Under HAZ, the microstructure of ultra-high strength low-alloy steel 30CrMnSiNi2A is composed of pearlites and ferrites.

3 Discussion

3.1 Microstructure

Table 4 shows the relationship between γ -(Ni, Fe) dendrite refinement and La content percentage in coatings. With the depth increasing from label 1 to 3, the La percentage decreases from 0.048 to 0.015; meantime volume of dendrite grain grows significantly.

The grain refinement of La_2O_3 can be illustrated as two parts. Firstly, the RE doped in coatings increases the solidification temperature which induces the decrease of solidification temperature range. La suppresses the ripening and coarsening of secondary dendrites. Secondly, the La_2O_3 possesses a high melting point of 2500 °C. Therefore in laser cladding this leads to a nucleating agent effect, nucleation sites increment, interfacial energy reduction and growth retardance on Ni solid-solution grains in cooling^[7,18].

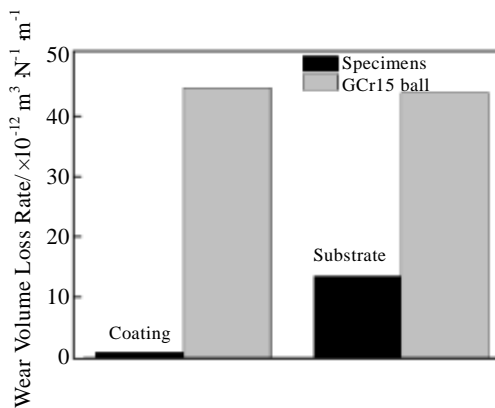


Fig.8 Wear rate as a function of dry sliding at 25 N

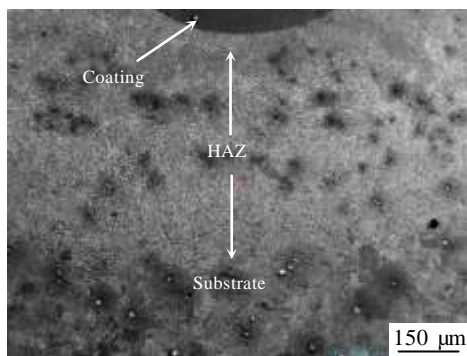


Fig.9 SEM image of HAZ

Finally, in addition to promoting the formation of a fine dendrite, La has also the effect of desulfurization. RE element reacts with sulfur to form low density and high incipient melting temperature sulfides in melting^[15]. Big La atoms with radius 0.1877 nm and active chemical properties attract sulfurs and phosphorus around them, the majority of low density compounds swimming to the surface of melt pool and some remaining between dendrites surfaces before solidifying. This process purifies Ni solid solution and brings excellent toughness for Ni-based alloy coating. La increases the density of grain boundary and suppresses grain growth thus refining grain size. Further refinement of grain size is caused by laser processing, great cooling rate related to high temperature gradient between laser radiated substrate zone and the non-radiated low temperature region.

Theories which try to explain the effect of RE addition on grain refining, structural purifying and enhancement of solid solution can be summarized as the following three aspects: (1) The spontaneous nucleation of high melting point compounds produced by RE purifying effect effectively refines columnar grains and improves the morphology of acicular structure, and thus the mechanical properties of composite coatings can be enhanced^[9,19]. (2) RE has good solubility in Ni-based alloy and its intermetallic compounds cause solid solution strengthening. (3) Dispersively distributed RE compounds bonded well with matrix materials, not only stabilize grain boundary and eliminate the harmful sulfide and phosphide there, but also decrease alloy element diffusion velocity, thus slowing down the surface oxidation rate^[7-12,17].

3.2 Wear resistance

The abrasive wear mechanism can be understood in Fig.10. The exposed reinforcing phase causes a local abrasive wear action on GCr15 counter surface during the sliding test. Thus a protective transfer layer formed by GCr15 steel fragments exists between composite and GCr15 surface. It can be seen that there are only micro ploughing and spalling in Fig.10, no sever damage in composite coating surface. The lanthanum oxide addition improves Ni60A- La_2O_3 coatings surface wear resistance by dendrite growth constraint.

Table 4 EPMA point quantification analysis of locations labeled 1~3 in Fig.1 (wt%)

Element	Label 1	Label 2	Label 3
B	2.601	2.251	2.086
C	3.4	5.042	5.009
O	-	-	-
Si	1.487	1.279	1.645
Cr	9.567	9.999	9.054
Fe	54.378	54.836	53.805
Ni	28.519	26.564	28.386
La	0.048	0.029	0.015

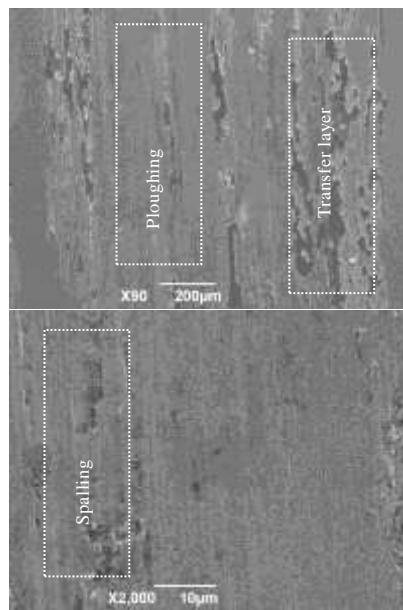


Fig.10 SEM images of worn surface

4 Conclusions

1) La_2O_3 addition significantly refines and purifies the microstructure of γ -(Ni, Fe) dendrite and interdendrite.

2) The hardness and wear properties of Ni60A-La coatings are significantly improved by dendrite refinement of La.

3) The dendrites size in top surface of laser coatings are finer than that in coating/substrate interface zone. It is caused by higher La density in coating surface.

4) A good macro- and microstructure composite Ni60A-La coating has been produced on super high strength steel 30CrMnSiNi2A.

5) A layer of high microhardness zone beneath the coating/substrate interface in substrate super high strength steel 30CrMnSiNi2A appears because of laser reheating.

References

- Paul C P, Mishra S K, Tiwari P et al. *Optics & Laser Technology*[J], 2013, 50: 155
- Ocelik V, Matthews D, De Hosson J T M et al. *Surface & Coatings Technology*[J], 2005, 197(2-3): 303
- Desale G R, Paul C P, Gandhi B K et al. *Wear*[J], 2009, 266(9-10): 975
- St-Georges L. *Wear*[J], 2007, 263(1-6): 562
- Amado J M, Tobar M J, Alvarez J C et al. *Applied Surface Science*[J], 2009, 255(10): 5553
- Amado J M, Montero J, Tobar M J et al. *Physics Procedia*[J], 2012, 39: 362
- Sharma S P, Dwivedi D K, Jain P K. *Wear*[J], 2009, 267(5-8): 853
- Farahmand P, Liu S, Zhang Z et al. *Ceramics International*[J], 2014, 40(10): 15 421
- Zhang S H, Li M X, Yoon J H et al. *Materials Chemistry and Physics*[J], 2008, 112(2): 668
- Zhou X W, Shen Y F. *Surface & Coatings Technology*[J], 2014, 249: 6
- Sen Ranjan, Das Siddhartha, Das Karabi. *Surface & Coatings Technology*[J], 2011, 205(13-14): 3847
- Cai B, Tan Y F, Tan H et al. *Transactions of Nonferrous Metals Society of China*[J], 2013, 23(7): 2002
- Zhang K M, Zou J X, Li J et al. *Transactions of Nonferrous Metals Society of China*[J], 2012, 22(8): 1817
- Li X L, He S M, Zhou X T et al. *Materials Characterization*[J], 2014, 95: 171
- Xiao C B, Han Y F. *Journal of Materials Science*[J], 2001, 36(4): 1027
- Song S H, Sun H J, Wang M. *Journal of Rare Earths*[J], 2015, 33(11): 1204
- Serres Nicolas, Hlawka Françoise, Costil Sophie et al. *Wear*[J], 2011, 270(9-10): 640
- Wang K L, Zhang Q B, Sun M L et al. *Applied Surface Science*[J], 2001, 174(3-4): 191
- Farahmand Parisa, Kovacevic Radovan. *Surface & Coatings Technology*[J], 2015, 276: 121

激光熔覆纳米 La_2O_3 添加镍基合金涂层的显微组织与耐磨性研究

赵宁^{1,2}, 陶礼^{1,2}, 郭辉^{1,2}, 张蒙祺^{1,2}

(1. 西北工业大学, 陕西 西安 710072)

(2. 陕西省机电传动与控制工程实验室, 陕西 西安 710072)

摘要: 以激光工艺制备了添加纳米 La_2O_3 初料的镍基涂层。激光熔覆之前, 高能球磨机充分混合的Ni60A和 La_2O_3 粉床预置于基体30CrMnSiNi2A表面。La偏聚于枝晶间从而限制了二次枝晶的成长和熟化。显微组织得到了细化。由于更高的La富集, 涂层上表面显微组织细化更为显著, 这一现象的上述解释得到EPMA结果佐证。熔覆涂层经过RE显微组织细化和净化, 硬度、耐磨性均相对基体金属显著提升, 而涂层中裂纹和孔隙均未出现。涂层的摩擦系数曲线COF明显低于基体, 磨擦体积损失率和显微硬度值分别是基体数值的1/10和4倍。

关键词: 镍基合金涂层; La_2O_3 ; 激光熔覆; 显微组织细化; 摩擦磨损

作者简介: 赵宁, 男, 1958年生, 博士, 教授, 西北工业大学机电学院, 陕西 西安 710072, 电话: 029-88460507, E-mail: npuzhaon@163.com